

On the steady states of the spherically symmetric Einstein-Vlasov system

Håkan Andréasson
Department of Mathematics, Chalmers,
S-41296 Göteborg, Sweden
email: `hand@math.chalmers.se`

Gerhard Rein
Department of Mathematics, University of Bayreuth,
D-95440 Bayreuth, Germany
email: `gerhard.rein@uni-bayreuth.de`

August 29, 2018

Abstract

Using both numerical and analytical tools we study various features of static, spherically symmetric solutions of the Einstein-Vlasov system. In particular, we investigate the possible shapes of their mass-energy density and find that they can be multi-peaked, we give numerical evidence and a partial proof for the conjecture that the Buchdahl inequality $\sup_{r>0} 2m(r)/r < 8/9$, $m(r)$ the quasi-local mass, holds for all such steady states—both isotropic *and* anisotropic—, and we give numerical evidence and a partial proof for the conjecture that for any given microscopic equation of state—both isotropic *and* anisotropic—the resulting one-parameter family of static solutions generates a spiral in the radius-mass diagram.

1 Introduction

When studying the properties of non-vacuum spacetimes in general relativity the choice of the matter model is important. In the present paper matter is described as a large ensemble of particles which interact only via the gravitational field created by the particles themselves and not via collisions between them. The distribution of the particles on phase space is given

by a distribution function f . This function satisfies the Vlasov equation, a first order conservation law the characteristics of which are the geodesics of the spacetime metric, and on the other hand f gives rise to macroscopic quantities such as mass-energy density, pressure, and mass current which act as source terms in the Einstein field equations. For an introduction to kinetic theory in general relativity and the Einstein-Vlasov system in particular we refer to [1] and [16].

One distinguishing feature of the Einstein-Vlasov system is that it allows for a wide variety of static solutions. The purpose of the present paper is to analyze spherically symmetric static solutions both numerically and analytically. After some general discussion of such steady states in the next section and a brief discussion of our numerical approach we investigate three different features of the steady states. In Section 3 the energy density as a function of the area radius is characterized into three distinct classes. In particular, we study steady states which as a function of the area radius are supported in an interval $[R_0, R_1]$ with $R_0 > 0$, which we call shells, as well as states supported in $[0, R_1]$, which we call non-shells. One observation is that anisotropic steady states can have a quite rich structure, in particular when compared with their Newtonian analogues, the steady states of the Vlasov-Poisson system. For instance, the energy density can have arbitrarily many peaks and in the case of shells these can be separated by vacuum regions so that the steady states consist of rings of Vlasov matter.

Then we consider the question whether there is an upper bound strictly smaller than 1 of the quantity $2M/R_1$, where M is the ADM mass. For *isotropic* perfect fluid solutions which satisfy the hypothesis that the energy density is non-increasing outwards the inequality

$$\frac{2M}{R_1} < \frac{8}{9}, \tag{1.1}$$

was shown by Buchdahl [7]. We prove a pointwise version of this inequality, cf. inequality (4.5) below, for a class of steady states of the Einstein-Vlasov system which includes, but is not restricted to, isotropic states. Moreover, we give numerical evidence for the conjecture that all spherically symmetric steady states of the Einstein-Vlasov system satisfy this inequality, even if the energy density is not radially non-increasing. We mention in passing that the inequality is sharp in the case of shells, cf. [2].

If one prescribes the microscopic equation of state, i.e., the way in which f depends on the local energy and angular momentum, one obtains a one parameter family of steady states. In the last section we investigate the relation of the ADM mass to the outer area radius of the steady state along

such one-parameter families. We prove the existence of mass-radius spirals for the isotropic case by reducing it to a result of Makino [11] for isotropic fluids, and we give numerical evidence that these radius-mass spirals are present for any microscopic equation of state, independently of isotropy, a feature which is again in sharp contrast to the Newtonian situation.

2 Static solutions of the spherically symmetric Einstein-Vlasov system

In Schwarzschild coordinates the metric of a static spherically symmetric spacetime takes the form

$$ds^2 = -e^{2\mu(r)} dt^2 + e^{2\lambda(r)} dr^2 + r^2(d\theta^2 + \sin^2\theta d\varphi^2),$$

where $r \geq 0$, $\theta \in [0, \pi]$, $\varphi \in [0, 2\pi]$. Asymptotic flatness is expressed by the boundary conditions

$$\lim_{r \rightarrow \infty} \lambda(r) = \lim_{r \rightarrow \infty} \mu(r) = 0,$$

and a regular centre requires

$$\lambda(0) = 0. \tag{2.1}$$

The static Einstein-Vlasov system is given by the Einstein equations

$$e^{-2\lambda}(2r\lambda' - 1) + 1 = 8\pi r^2 \rho, \tag{2.2}$$

$$e^{-2\lambda}(2r\mu' + 1) - 1 = 8\pi r^2 p, \tag{2.3}$$

together with the static Vlasov equation which can be written as

$$w \partial_r f - ((1 + w^2 + L/r^2)\mu' - L/r^3) \partial_w f = 0. \tag{2.4}$$

The variables w and L can be thought of as the momentum in the radial direction and the square of the angular momentum respectively. The matter quantities are given by

$$\rho(r) = \frac{\pi}{r^2} \int_{-\infty}^{\infty} \int_0^{\infty} \sqrt{1 + w^2 + L/r^2} f(r, w, L) dL dw, \tag{2.5}$$

$$p(r) = \frac{\pi}{r^2} \int_{-\infty}^{\infty} \int_0^{\infty} \frac{w^2}{\sqrt{1 + w^2 + L/r^2}} f(r, w, L) dL dw, \tag{2.6}$$

where ρ denotes the mass energy density and p is the radial pressure.

Before we discuss how solutions of this system can be obtained we note some additional equations which follow from the above. Let the quasi-local mass be defined by

$$m(r) := 4\pi \int_0^r s^2 \rho(s) ds. \quad (2.7)$$

The ADM mass is then $M = \lim_{r \rightarrow \infty} m(r)$. Using m , the field equation (2.2) together with the boundary condition (2.1) imply that

$$e^{-2\lambda(r)} = 1 - \frac{2m(r)}{r}, \quad (2.8)$$

and by (2.3),

$$\mu'(r) = e^{2\lambda(r)} \left(\frac{m(r)}{r^2} + 4\pi r p(r) \right). \quad (2.9)$$

In particular, μ is radially increasing. Eqns. (2.2) and (2.3) are the 00 and 11 components of the Einstein field equations, and given the matter quantities they together with the boundary conditions suffice to determine the metric. But the 33 component of the Einstein equations is also non-trivial and reads

$$e^{-2\lambda} (\mu'' + (\mu' + 1/r)(\mu' - \lambda')) = 8\pi p_T, \quad (2.10)$$

where the tangential pressure p_T is given by

$$p_T(r) = \frac{1}{2} \frac{\pi}{r^4} \int_{-\infty}^{\infty} \int_0^{\infty} \frac{L}{\sqrt{1 + w^2 + L/r^2}} f(r, w, L) dL dw. \quad (2.11)$$

Eqn. (2.10) follows from (2.2)–(2.6); the also non-trivial 44 component is a multiple of the former. Next we note that the Tolman-Oppenheimer-Volkoff equation

$$p' = \frac{2}{r}(p_T - p) - \mu'(\rho + p) \quad (2.12)$$

holds for any sufficiently regular static solution of the spherically symmetric Einstein-Vlasov equation, as can be seen by a simple computation, using (2.4) to express p' . Finally, if we add (2.2) and (2.3) we obtain the identity

$$\lambda' + \mu' = 4\pi r e^{2\lambda} (\rho + p). \quad (2.13)$$

Let us now briefly discuss how one can establish the existence of static solutions of the spherically symmetric Einstein-Vlasov system; for more details we refer to [12, 13, 14, 15]. Let

$$E := e^{\mu(r)} \sqrt{1 + w^2 + L/r^2}$$

denote the local or particle energy which like L is conserved along characteristics of the static Vlasov equation (2.4). The ansatz

$$f(r, w, L) = \Phi(E, L) \tag{2.14}$$

satisfies the Vlasov equation, and the macroscopic matter quantities become functionals of the metric coefficient μ . Substituting these into Eqn. (2.9) and using (2.8) the above system reduces to a single first order equation for μ . Analyzing the latter constitutes an efficient way to prove the existence of static solutions with finite ADM mass and finite extension. It should be pointed out that spherically symmetric static solutions which do not globally have the form (2.14) exist, cf. [17]. This contrasts the Newtonian case where all spherically symmetric static solutions have the form (2.14), a fact known as Jeans' Theorem, cf. [5]. As a matter of fact, below we obtain steady states which are good candidates for solutions which are not globally of the form (2.14).

In [15, Thm. 2.1] it has been shown that in order to obtain a steady state of finite ADM mass by the above approach there must exist a cut-off energy E_0 such that $\Phi(E, L) = 0$ for $E > E_0$ and $L \geq 0$. If Φ and in particular such a cut-off energy is prescribed we obtain a steady state solution by prescribing $\mu(0)$ and solving—numerically or analytically—the resulting equation (2.9) radially outward. However, the resulting solution will in general not satisfy the boundary condition $\mu(\infty) = 0$, but it will have some finite limit $\mu(\infty)$. One can then shift both the cut-off energy and the solution by this limit to obtain a solution which satisfies the boundary condition $\mu(\infty) = 0$. This does not affect m and hence also not λ , where it should be noted that the boundary conditions for the latter both at the centre and at infinity follow from (2.8), provided that the solution has finite ADM mass and that ρ is not too singular at the centre.

As long as one is interested in only a single steady state at a time this way of handling the boundary condition for μ at infinity is acceptable, but it is awkward when one studies families of such steady states, since E_0 and $\mu(0)$ cannot be treated as two free parameters if one insists on the boundary condition at infinity. Hence we found it convenient to use an ansatz where the resulting equation for μ can be rewritten in terms of the function $y(r) = e^{\mu(r)}/E_0$. The following is sufficiently general for our purposes:

$$f(r, w, L) = \phi(E/E_0)(L - L_0)_+^l, \tag{2.15}$$

where $l > -1/2$, $E_0 > 0$, $L_0 \geq 0$, $x_+ := \max\{x, 0\}$ denotes the positive part, and $\phi :]0, \infty[\rightarrow]0, \infty[$ is measurable, $\phi(\eta) = 0$ for $\eta > 1$, and there exist

constants $k > -1$ and $C > 0$ such that

$$\phi(\eta) \leq C(1 - \eta)^k, \quad \eta \in]0, 1[.$$

With the ansatz (2.15),

$$\rho(r) = c_l r^{2l} (1 + L_0/r^2)^{l+2} (g_{l+3/2} + g_{l+1/2}) (\sqrt{1 + L_0/r^2} y(r)), \quad (2.16)$$

$$p(r) = \frac{c_l}{2l+3} r^{2l} (1 + L_0/r^2)^{l+2} g_{l+3/2} (\sqrt{1 + L_0/r^2} y(r)), \quad (2.17)$$

$$p_T(r) = (l+1)p(r) + \frac{c_l}{2} L_0 r^{2l-2} (1 + L_0/r^2)^{l+1} g_{l+1/2} (\sqrt{1 + L_0/r^2} y(r)),$$

where for $j > -1$, $l > -1$, and $u \in]0, 1]$,

$$g_j(u) := \int_1^{1/u} \phi(u\eta) (\eta^2 - 1)^j d\eta = u^{-(2j+1)} \int_u^1 \phi(\eta) (\eta^2 - u^2)^j d\eta, \quad (2.18)$$

$g_j(u) := 0$ for $u > 1$, and

$$c_l := 2\pi \int_0^1 s^l (1-s)^{-1/2} ds.$$

The equation to be solved for y then becomes

$$y' = \frac{y}{1 - \frac{2m(r,y)}{r}} \left(\frac{m(r,y)}{r^2} + 4\pi r p(r,y) \right), \quad (2.19)$$

where the dependence of m and p on y arises via the above formulas (2.16) and (2.17).

In this way the cut-off energy E_0 disappears as a free parameter of the problem, and for ϕ , l , and L_0 fixed we obtain a one-parameter family of solutions parameterized by $y(0) > 0$. Once y is determined on the support of the solution its limit $y(\infty)$ at infinity can be computed, and if we define $E_0 := 1/y(\infty)$ and $e^{\mu(r)} := E_0 y(r)$ we have a steady state with the proper boundary condition at infinity.

Notice that if $l = 0 = L_0$, i.e., the microscopic equation of state (2.15) does not depend on angular momentum, then $p_T = p$, i.e., tangential and radial pressure are equal, which is why such steady states of the Einstein-Vlasov system are called *isotropic*.

If $j > -1$ and $k + j + 1 > 0$ then $g_j \in C([0, \infty[)$. If $j > 0$ and $k + j > 0$ then $g_j \in C^1([0, \infty[)$ with

$$g'_j(u) = -\frac{1}{u} ((2j+1)g_j(u) + 2jg_{j-1}(u)), \quad (2.20)$$

cf. [15, Lemma 2.2]. With this regularity of the matter terms as functions of y it is easy to see that Eqn. (2.19) has for any choice of $y(0) > 0$ a unique solution. The non-trivial question is which choices for ϕ lead to steady states of finite ADM mass and finite extension. In [15, Thm. 3.1] it has been shown that this is the case if $L_0 = 0$ and

$$\phi(\eta) = c(1 - \eta)^k + O((1 - \eta)^{k+\delta}) \text{ as } \eta \rightarrow 1- \quad (2.21)$$

where $c > 0$, $\delta > 0$, and $k, l \in \mathbb{R}$ are such that

$$k > -1, \quad l > -\frac{1}{2}, \quad k + l + \frac{1}{2} > 0, \quad k < l + \frac{3}{2}.$$

In this case the resulting steady state is non-trivial iff $y(0) \in]0, 1[$.

To conclude this section we briefly discuss how we construct the steady states numerically. If an ansatz of the form (2.15) is given, the value of the integral $g_j(u)$ and hence of ρ and p as functions of r and $y(r)$ can easily be computed. In practice we preferred to choose ansatz functions of the form

$$f(r, w, L) = (1 - E/E_0)_+^k (L - L_0)_+^l, \quad (2.22)$$

with $k \geq 0$, $l > -1/2$, $k < 3l + 7/2$, $E_0 > 0$, $L_0 \geq 0$, and k, l such that the relevant integrals g_j can be computed explicitly by hand. In [13] it has been shown that such an ansatz leads to finite ADM mass and compact support as well. In the Newtonian case with $l = L_0 = 0$, this ansatz gives steady states with a polytropic equation of state. With ρ and p then given as functions of r and $y(r)$ we use a simple Euler-type or a leap-frog scheme to solve the equation (2.19), starting with some prescribed value $y(0) \in]0, 1[$ at the centre and moving with a fixed step size Δr radially outward. If we are in a situation where the rigorous results cited above guarantee that the solution has a finite extension, the expression $\sqrt{1 + L_0/r^2}y(r)$ exceeds the threshold 1 for sufficiently large values of r . Once this happens the computation can be stopped, and the spacetime can be extended by an exterior Schwarzschild solution of the appropriate ADM mass.

It should be noted that when $L_0 > 0$ the expression $\sqrt{1 + L_0/r^2}y(r)$ will always exceed 1 for sufficiently small values of r , and there will be no matter in the region

$$r < \sqrt{\frac{L_0}{y(0)^{-2} - 1}} =: R_0. \quad (2.23)$$

In this case y is constant in the inner vacuum region $[0, R_0]$, and we start our numerical computation at the radius R_0 . The choice $L_0 > 0$ also leads to

another complication, since in that case the support of the solution may in general consist of several concentric shells, a feature which is not captured if the computation is stopped the first time that $\sqrt{1 + L_0/r^2}y(r)$ again exceeds 1.

3 Characterization of steady states

In this section we are interested in the possible shapes of the energy density ρ and its support. In particular we will numerically construct multi-peaked steady states which seem to have no analogue in the Newtonian situation.

We start with some simple analytic observations. Without explicitly mentioning it we only consider non-trivial steady states of finite ADM mass and compact support. In particular, $m(r) > 0$ for some area radius r , and hence $m > 0$ on an interval of the form $]R_0, \infty[$ where $R_0 \geq 0$ is given by (2.23). Notice that if $L_0 > 0$ then at $r = R_0$ by definition $y\sqrt{1 + L_0/r^2} = 1$, and $\frac{d}{dr}y\sqrt{1 + L_0/r^2} = -y(1 + L_0/r^2)^{-1/2}L_0/r^3 < 0$ so that $y\sqrt{1 + L_0/r^2} < 1$ on some interval of the form $]R_0, R_0 + \delta[$.

Observation 3.1. The function y is constant on $[0, R_0]$ and strictly increasing on $[R_0, \infty[$. This follows immediately from (2.19).

Observation 3.2. If the solution is isotropic, i.e., $l = 0 = L_0$, then ρ is strictly decreasing and its support is an interval of the form $[0, R_1]$.

Observation 3.3. If $L_0 = 0$, then the support of the solution is still an interval of the form $[0, R_1]$. This follows from Observation (3.1), Eqn. (2.16), and the strict monotonicity of the functions g_j on their support, cf. (2.20). Note however that in the anisotropic case $l \neq 0$ the energy density ρ is in general no longer monotone.

Observation 3.4. If $L_0 > 0$, then we have vacuum in the interval $[0, R_0]$, $m(r) > 0$ for $r > R_0$, and the support is contained in some interval $[R_0, R_1]$. As we shall see below the support will in general no longer be a single interval.

Steady states which are supported in $[R_0, R_1]$ with $R_0 > 0$ we call shells, and states with $R_0 = 0$ we call non-shells. In Section 3.3 below we give a quite general characterization of both shells and non-shells for different values of the parameters k, l, L_0 and $y(0)$. The main focus in that section is on cases which have rather small values on $y(0)$ since this is a necessity for obtaining several peaks. In the following sections we have chosen to study shells and non-shells separately for values of $y(0)$ which give no more than two peaks. One reason for this is that it is then easier to visualize the large

difference in magnitude of the first peak compared to the following one for these values of $y(0)$; in Section 3.3 we really use the quantity $4\pi r^2 \rho$ rather than ρ itself and moreover we use a logarithmic scale in order to get more informative pictures for the multi-peaks. The second reason is that we want to emphasize the important feature that shells can have separating vacuum regions whereas non-shells cannot, and we find that this point is made more clear by first splitting the presentation into shells and non-shells.

3.1 Shells

Since the main purpose of this and the next section is to emphasize a couple of features of the shape of the energy density which are present for any choice $k \geq 0$ and $l \geq 0$ when $L_0 > 0$, we fix $k = 0$, $l = 1.5$, and $L_0 = 0.2$. A more general analysis where the influence of all parameters is taken into account is carried out in Section 3.3 below.

Let us for these values of k , l , and L_0 compute steady states with three different values of $y(0)$, namely $y(0) = 0.4$, 0.22 , 0.12 . We find that these

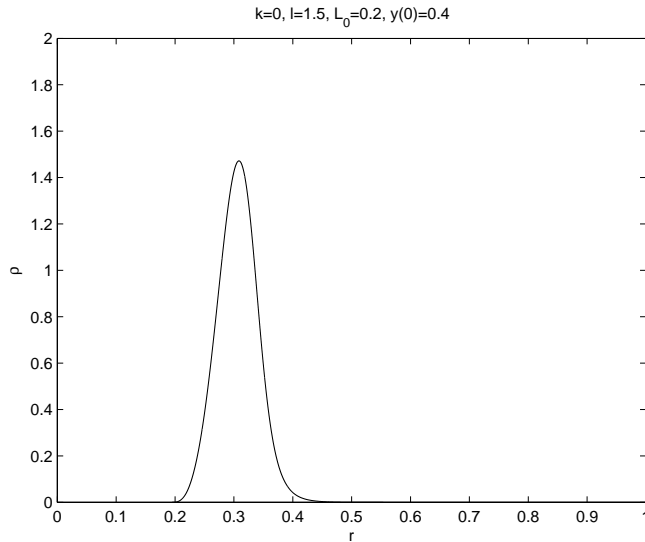


Figure 1: A pure shell

values give rise to three distinct states. When $y(0) = 0.4$ we get a pure shell, i.e., the energy density increases, reaches a maximum value and then decreases to zero and remains zero for all larger values on r . In the second

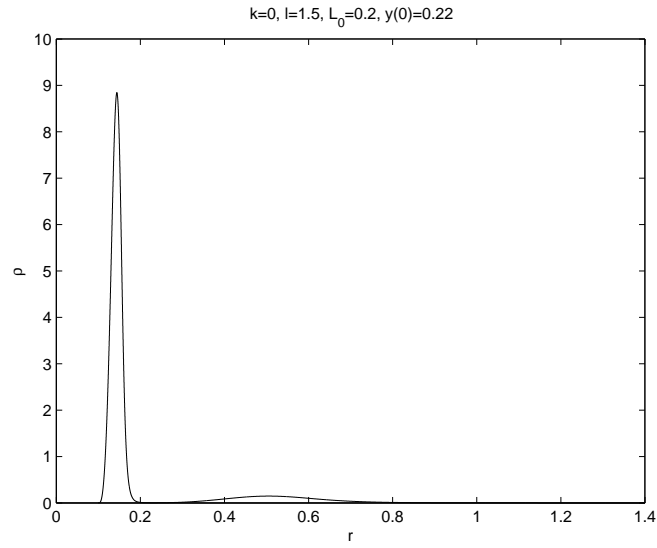


Figure 2: A shell with a tail

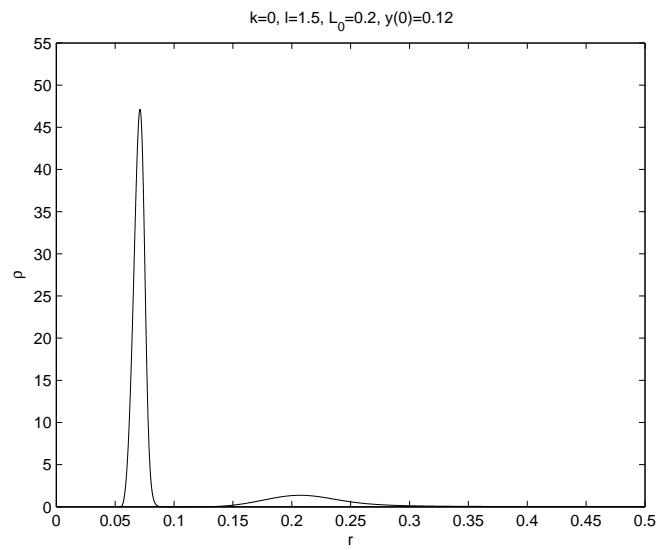


Figure 3: A vacuum region before the tail

situation, when $y(0) = 0.22$, the maximum value of ρ is followed by a local minimum, strictly greater than zero (this is hard to see in the figure but is easy to check in the data file), and then a tail with a small amplitude, relative to the maximum value, but with a considerable extension. In the final case, where $y(0) = 0.12$, there is a vacuum region between the first part, which is a pure shell, and the tail. In this case a Schwarzschild solution can be joined at the first point where the energy density vanishes which results in a different steady state, a pure shell.

We point out that in [2] it is indeed proved that the energy density vanishes close to R_0 if $y(0)$ is small which corresponds to the third case above. Furthermore, in Section 2 we mentioned that Jeans' Theorem does not hold for the Einstein-Vlasov system, cf. [17], and the distribution function f of the steady state obtained by joining a Schwarzschild solution as described above for $y(0) = 0.12$ is not globally given as *one* function of E and L as in the ansatz (2.14).

3.2 Non-shells

In the case when $L_0 = 0$, the energy density can be strictly positive or vanish at $r = 0$ (depending on l) but it is always strictly positive sufficiently close to $r = 0$. Hence, the support of the matter is an interval $[0, R_1]$ with $R_1 > 0$, and we call such states non-shells. From Observation 3.3 it follows that no vacuum region can separate two parts of a non-shell. Except for this fact, the basic features of the shape of the energy density are preserved for non-shells. In Figures 4 and 5 the energy densities of two non-shells are shown, corresponding to $k = 0$, $l = 1.5$, $y(0) = 0.4$ and $k = 0$, $l = 5.5$, $y(0) = 0.1$. We see that these have very similar features as the shells in Figures 1 and 2. Again we note (cf. Figure 5) the large difference in amplitude of the first peak compared to the second one. In view of Observation 3.3, which implies that $\rho > 0$ in $[0, R_1]$, it is interesting to note that non-shells nevertheless mimic the behaviour of shells close to $r = 0$, cf. Figure 5, in the sense that the energy density almost vanishes on an interval $[0, R_0]$, for some small $R_0 > 0$.

Below we will see that the number of peaks is in general not restricted to two as in Figures 2, 3, and 5. However, numerically we found that already these solutions with two peaks seem to have no analogue for the Vlasov-Poisson system.

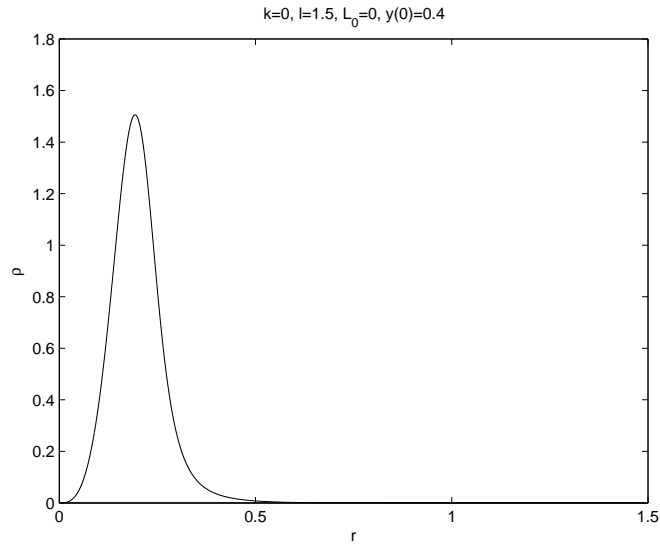


Figure 4: A non-shell without a tail

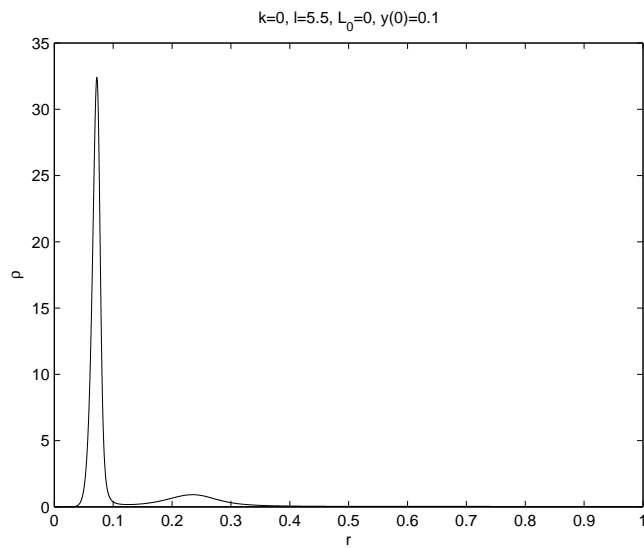


Figure 5: A non-shell with a tail

3.3 Multi-peaked steady states

In this section we construct solutions where the energy density has many peaks, and we give numerical evidence that there is no limit to the number of the peaks. Instead of plotting the energy density ρ itself we plot $\tilde{\rho} = 4\pi r^2 \rho$ (or the logarithm of this quantity) since the pictures become clearer due to the fact that the first peak which in amplitude is completely dominating gets reduced due to the factor r^2 . In general the amplitude of the peaks get smaller as r increases and thus the quantity $4\pi r^2 \rho$ shows less difference between the peaks and the resolution in the pictures is improved, but we point out that the important features of ρ are similar to those of $\tilde{\rho}$.

We have first chosen to study the non-shells, i.e., $L_0 = 0$. In Figure 6 the parameter $k = 0$ is fixed and the dependence upon l and $y(0)$ is depicted. We see that the parameter $y(0)$ has an important effect on the number of the peaks, eg. in the last row we get from two to four peaks by decreasing $y(0)$ from 0.2 to 0.05. Increasing the parameter l may also increase the number of peaks as seen in column 2 and 3. Also the peaks become more narrow as l is increased. We point out that more peaks are obtained by decreasing $y(0)$ further, cf. Figure 11 which shows a shell with $y(0) = 0.01$.

In Figure 7 we have fixed $l = 12$ and $y(0) = 0.05$ which corresponds to the final case in Figure 6, and we investigate the influence of k . We find that by increasing k the decay rate of $\tilde{\rho}$ is affected for large r and the peaks in general become wider as k is increased.

Let us now turn to the shells. We first fix $k = 1$, $l = 1$, and $L_0 = 3$ and vary $y(0)$. The result is shown in Figure 8. It is instructive to compare this result with the upper row in Figure 6. We see that the influence of a non-vanishing L_0 increases the amplitude of $\tilde{\rho}$ and also more peaks are obtained. The results obtained by varying L_0 are then shown in Figure 9. First of all we notice that the number of peaks is affected, and we also note that the peaks get more narrow as L_0 increases. In particular we get in the case when $L_0 = 1.5$ one vacuum region which separates the first two peaks and in the case when $L_0 = 10$, there are two vacuum regions.

The dependence on l is shown in Figure 10 and a similar behaviour as in Figure 6 is found. Increasing l can give rise to new peaks and quite generally it makes the peaks more narrow.

Finally we show in Figure 11 a case where $k = 1$, $l = 10$, $L_0 = 3$, and $y(0) = 0.01$, which has ten peaks, and we note that there are three vacuum regions separating the first four peaks.

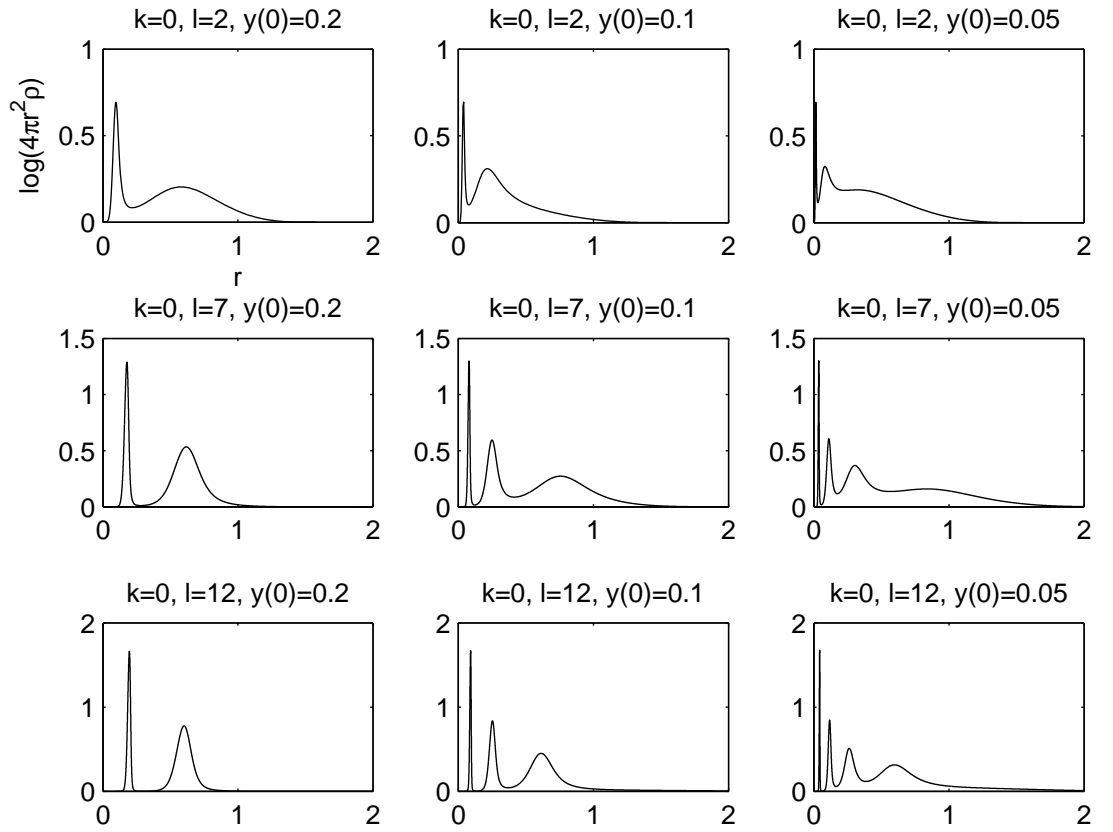


Figure 6: Multi-peaks of non-shells, $L_0 = 0$

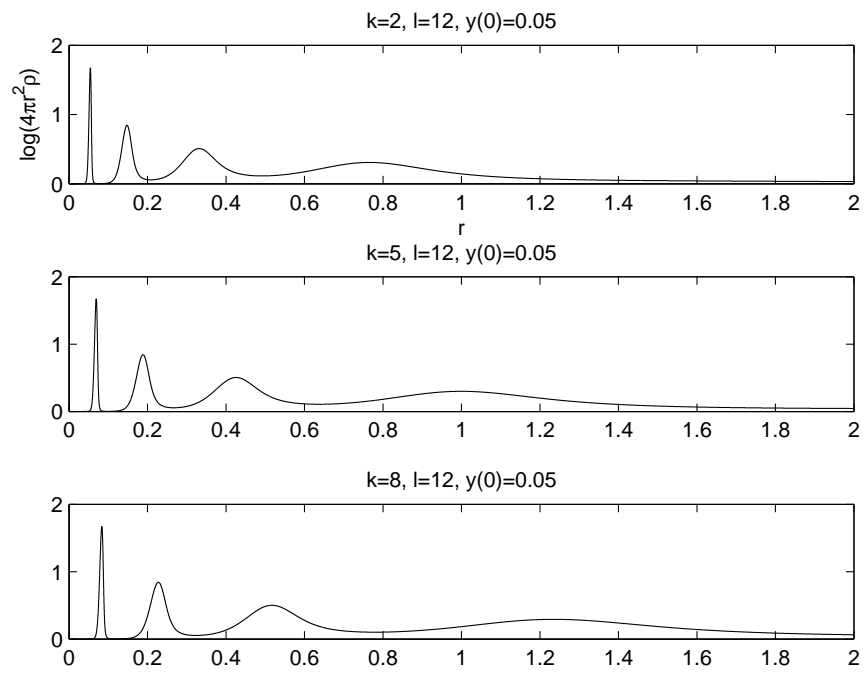


Figure 7: Multi-peaks of non-shells, $L_0 = 0$

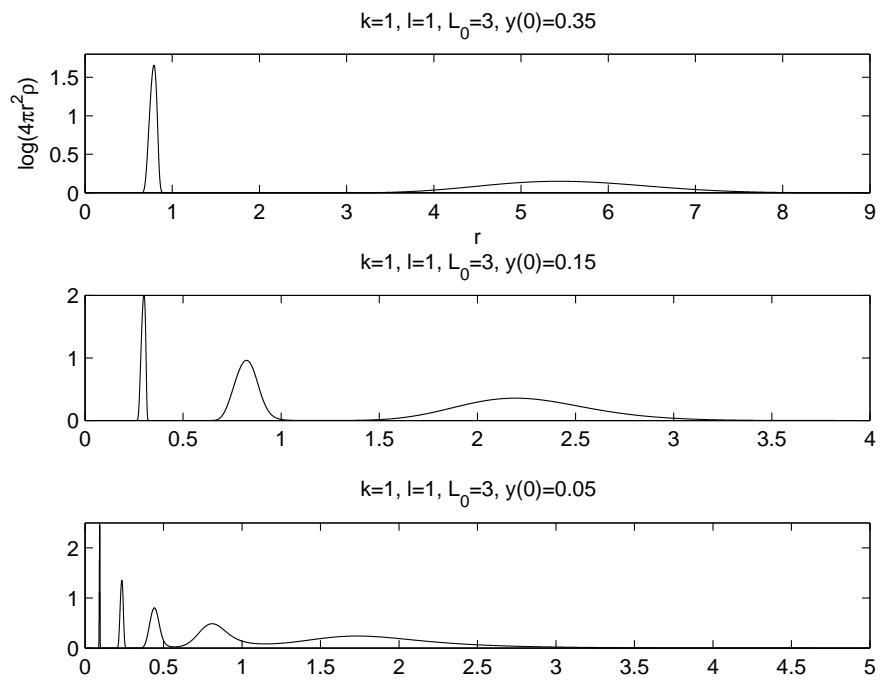


Figure 8: Multi-peaks of shells

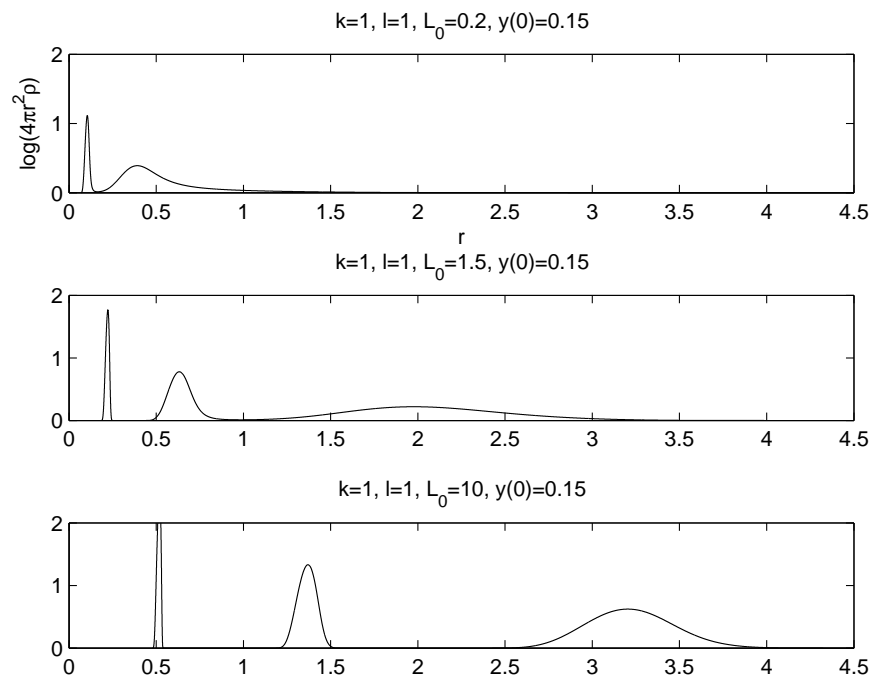


Figure 9: Multi-peaks of shells

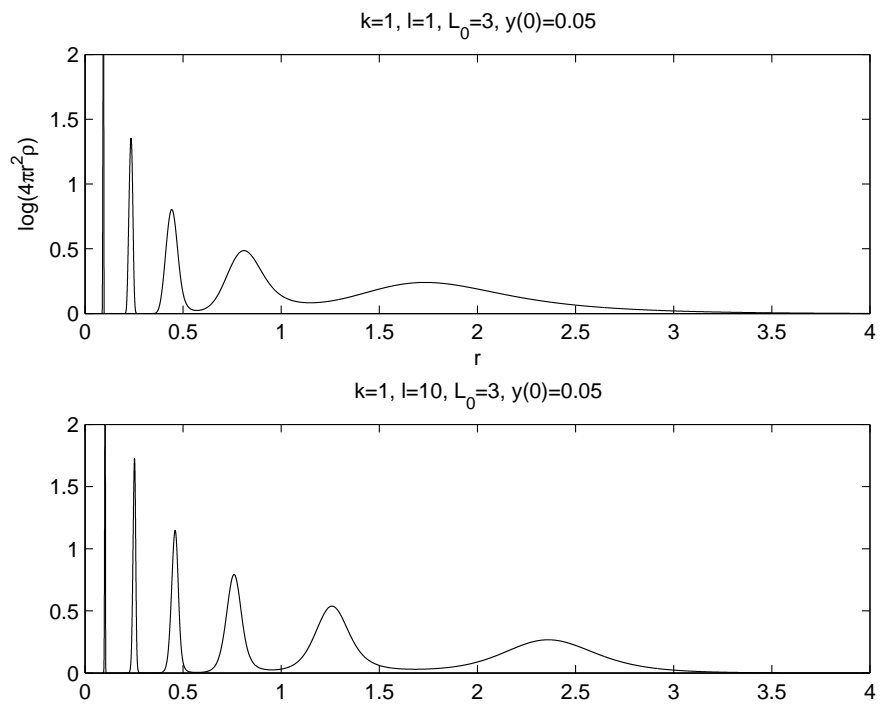


Figure 10: Multi-peaks of shells

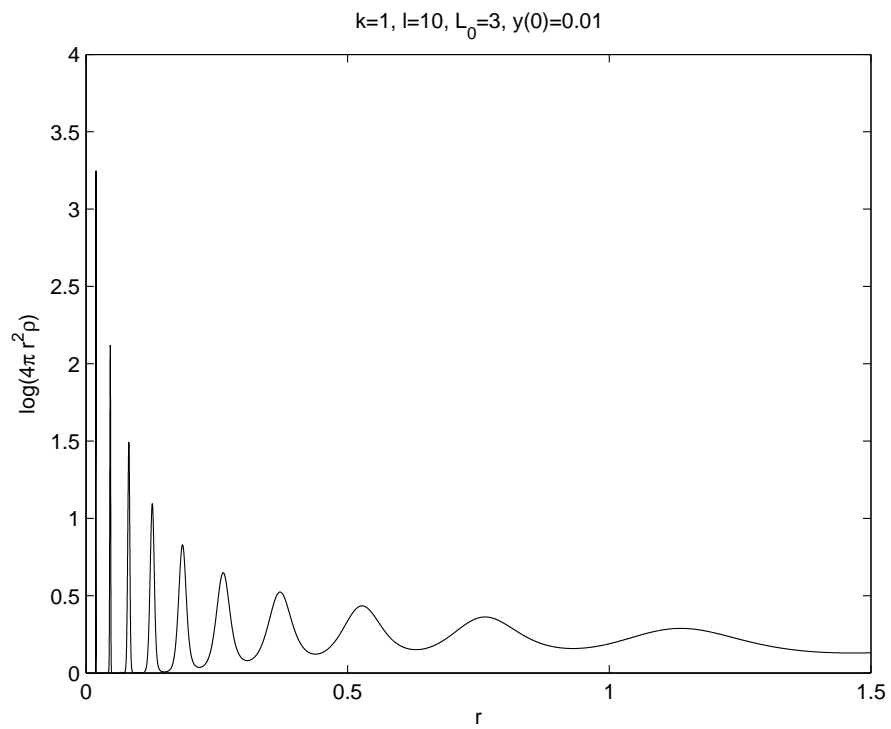


Figure 11: Multi-peaks of a shell

4 The Buchdahl inequality

Let us define

$$\Gamma := \sup_{r \geq 0} \frac{2m(r)}{r}. \quad (4.1)$$

In this section we investigate if Γ has an upper bound less than one for static solutions of the spherically symmetric Einstein-Vlasov system. We start with the following analytic result the proof of which is modeled on the original proof by Buchdahl.

Theorem 1 *The Buchdahl inequality*

$$\Gamma < \frac{8}{9}$$

holds for spherically symmetric steady states of the Einstein-Vlasov system which satisfy the condition that

$$p \geq p_T \text{ and } \rho \text{ is non-increasing.} \quad (4.2)$$

These assumptions are satisfied if $l = 0 = L_0$ in the ansatz (2.15), i.e., the steady state is isotropic, but also if $L_0 = 0$ and $l < 0$ in which case the steady state is anisotropic.

Proof. First of all we notice that using (2.13) the field equation (2.10) can be rewritten in the form

$$\frac{d}{dr} \left(r^2 e^{\mu-\lambda} \mu' \right) = 4\pi r^2 e^{\mu+\lambda} (\rho + p + 2p_T).$$

This equation is essentially the slicing condition for maximal areal coordinates which in the static case coincide with Schwarzschild coordinates, cf. [4]. Using (2.9) the above equation can be rewritten in the form

$$\frac{d}{dr} \left(\frac{1}{r} e^{\mu-\lambda} \mu' \right) = \frac{4\pi}{r} e^{\mu+\lambda} \left(\rho + 2p_T - \frac{3}{4\pi} \frac{m}{r^3} - 2p \right). \quad (4.3)$$

In the sequel we abbreviate $z(r) = m(r)/r^3$. Since ρ is non-increasing,

$$z(r) = \frac{4\pi}{r^3} \int_0^r \rho(s) s^2 ds \geq \frac{4\pi}{r^3} \rho(r) \int_0^r s^2 ds = \frac{4\pi}{3} \rho(r).$$

Since by assumption $p_T \leq p$, the function

$$\frac{1}{r} e^{\mu-\lambda} \mu'$$

is non-increasing. Since

$$z'(r) = -\frac{3}{r}z(r) + \frac{4\pi}{r}\rho(r) \leq 0,$$

the same is true for z . We now use

$$\xi = \xi(r) = 2 \int_0^r s e^{\lambda(s)} ds, \quad r \geq 0,$$

as a new independent variable and consider the function

$$\alpha(\xi) = e^{\mu(r)}.$$

Then

$$\frac{d\alpha}{d\xi} = e^{\mu(r)} \mu'(r) \frac{1}{2r e^{\lambda(r)}}$$

is non-increasing for $r > 0$ respectively $\xi > 0$. If we observe that Eqn. (2.8) can be rewritten as

$$e^{\lambda(r)} = (1 - 2r^2 z(r))^{-1/2}$$

then for $r > 0$,

$$\begin{aligned} \alpha(\xi(r)) &> \alpha(\xi) - \alpha(0) = \int_0^\xi \frac{d\alpha}{d\xi}(\zeta) d\zeta \\ &\geq \frac{d\alpha}{d\xi}(\xi)\xi = \frac{d\alpha}{d\xi}(\xi) \int_0^r 2s (1 - 2s^2 z(s))^{-1/2} ds \\ &\geq \frac{d\alpha}{d\xi}(\xi) \int_0^r 2s (1 - 2s^2 z(r))^{-1/2} ds \\ &= e^{\mu(r)} \mu'(r) \frac{1}{2r e^{\lambda(r)}} \frac{1}{z(r)} \left(1 - \sqrt{1 - 2r^2 z(r)}\right). \end{aligned}$$

By (2.9), $\mu'(r) \geq e^{2\lambda} r z(r)$, and inserting this into the previous estimate we find that

$$e^{\mu(r)} = \alpha(\xi(r)) > \frac{1}{2} e^{\mu(r)+\lambda(r)} (1 - e^{-\lambda(r)}).$$

This implies that $e^{\lambda(r)} < 3$ which is equivalent to the assertion on Γ .

For the ansatz (2.15) with $L_0 = 0$ and $l \leq 0$ the general assumptions used above are satisfied, and the proof is complete. \square

Remark. (a) The analysis above actually yields the somewhat sharper estimate that

$$e^{\mu(r)} - e^{\mu(0)} \geq \frac{1}{2} e^{\mu(r)} (e^{\lambda(r)} - 1),$$

and hence

$$\Gamma \leq 1 - \frac{1}{(3 - 2e^{\mu(0)})^2}.$$

(b) Although our numerical investigation indicates that the estimate $\Gamma < 8/9$ holds for steady states of the Einstein-Vlasov system in general, some key features used in the above proof fail, in particular, the right hand side of (4.3) is not negative in general. To see this, let

$$\tilde{\rho}(r) := r^{-2l}\rho(r), \quad \tilde{p}(r) := r^{-2l}p(r).$$

Then if $l > 0$ and $L_0 = 0$,

$$\begin{aligned} r^{-2l} \left(\rho + 2p_T - \frac{3}{4\pi} \frac{m}{r^3} - 2p \right) &= \tilde{\rho} + 2l\tilde{p} - \frac{3}{4\pi} \frac{m}{r^{3+2l}} \\ &\rightarrow \tilde{\rho}(0) + 2l\tilde{p}(0) - \frac{3}{3+2l}\tilde{\rho}(0) > 0 \end{aligned}$$

as $r \rightarrow 0$, and the right hand side of (4.3) is positive for r close to 0.

(c) In [9] bounds on Γ are considered under various assumptions. In particular the authors obtain the bound $8/9$ under the assumptions (4.2). We have chosen to include the above proof anyway for the sake of completeness and in order to stress the fact that for Vlasov matter these assumptions are satisfied for the ansatz (2.15) with $l \leq 0$ and $L_0 = 0$ so that steady states with these properties do exist. In [9] the authors also consider the general non-isotropic case without any monotonicity assumptions but instead they require that there is a constant B such that

$$\frac{(\rho - 3m/r^3) + 2(p_T - p)}{p + m/r^3} \leq B.$$

Under this assumption they obtain a bound on Γ which for large B can be written in the form

$$\Gamma \leq 1 - 2/(2 + B)^2.$$

As $B \rightarrow \infty$ this bound degenerates to the estimate $\Gamma \leq 1$. This is interesting in view of the numerical results presented below which indicate that Γ is *always* less than $8/9$, while the energy density along a family of steady states which makes Γ approach $8/9$ gets more and more peaked so that $B \rightarrow \infty$ (this is easily seen by considering an approximation of a Dirac measure). In the case of shells such a family has indeed been constructed for Vlasov matter and it has been shown that $\Gamma \rightarrow 8/9$ in that case, cf. [2]. We also refer to [3] where any matter model which satisfies $p + 2p_T \leq \Omega\rho$ is considered

($\Omega = 1$ for Vlasov matter) and where it is shown that a family of shells for which B can become arbitrary large satisfies $\Gamma \leq (2\Omega + 1)^2 - 1 / (2\Omega)^2$ so that Γ is strictly bounded away from one. Thus, as is shown in (b) above a proof of our general conjecture below must rely on mechanisms which are rather different from the ones in the proof of Theorem 1 and also different from [9].

Our next aim is to give numerical support to the conjecture that $\Gamma < 8/9$ holds for all spherically symmetric static solutions of the Einstein-Vlasov system. Our numerical study is restricted to distribution functions of the form (2.22). Since the qualitative behaviour is quite different in the case of shells and non-shells we will present the results for these cases separately.

4.1 Shells

In Figure 12 the values of Γ are shown for a family of steady states parameterized by $y(0) \in [0.03, 0.6]$. Here $k = 0$, $l = 3/2$, and $L_0 = 1$. We see that Γ stays below $8/9$. In Figure 13 we have changed the range of $y(0)$, namely $y(0) \in [e^{-14}, e^{-4}]$, in order to see that the family does approach $8/9$ as $y(0) \rightarrow 0$, which we know is the case by the result in [2]. This also provides a fairly tough test for our numerical scheme since the functions g_j become very large if y gets very close to 0.

We point out that the corresponding values of $2M/R_1$, where R_1 is the outer radius of the support would (as long as several peaks are present) be much less than Γ . This is clear in view of Section 3 where it was seen that the first peak is strongly dominating compared to the other peaks and most of the matter is captured in the first peak. Hence the value of r such that $\Gamma = 2m(r)/r$ is within that peak.

Let R_{11} be the outer radius of the *first* peak and consider the ratio R_{11}/R_0 as $y(0) \rightarrow 0$. We find in Figure 14 that $R_{11}/R_0 \rightarrow 1$ as $y(0) \rightarrow 0$. This fact is indeed proved in [2] and is crucial in order to show that $\Gamma \rightarrow 8/9$ for any family of shells for which $y(0) \rightarrow 0$.

In contrast to the non-shell case the behaviour of Γ for shells is qualitatively very similar for different values of k and l and we have therefore only included one case here. However we point out that all static shells that we have considered have satisfied $\Gamma < 8/9$.

4.2 Non-shells

In Figure 15 we depict Γ as a function of $y(0)$ for three different families of non-shells, where $l = 1, 5, 32$, and $k = 0$ in all cases. The results indicate

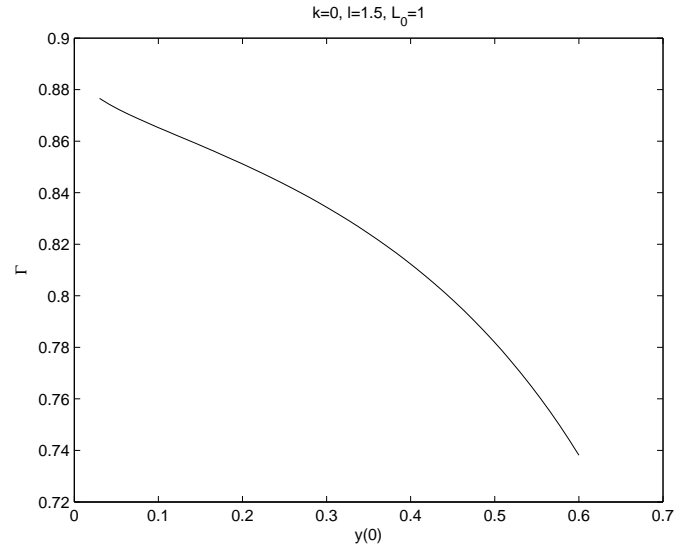


Figure 12: Γ versus $y(0)$ for shells

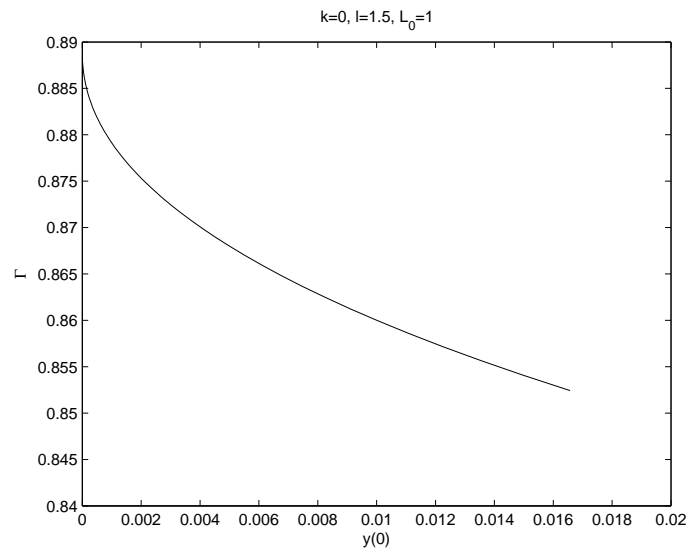


Figure 13: Γ versus $y(0)$ for shells

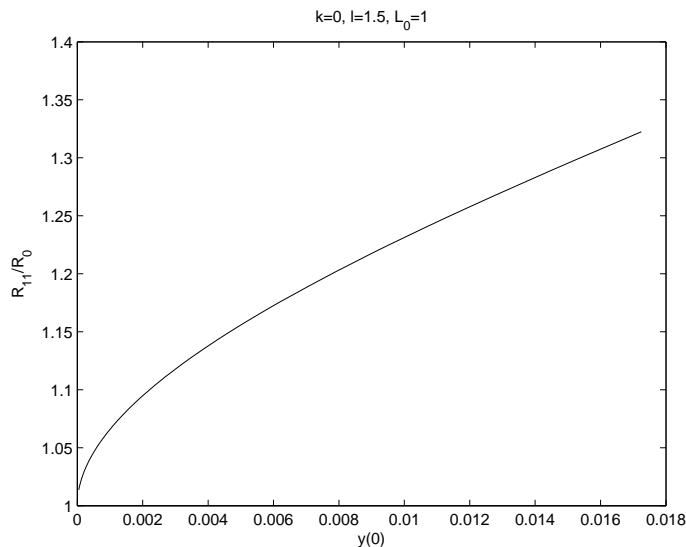


Figure 14: The ratio R_{11}/R_0

that

$$\Gamma < \kappa(l) < 8/9, \quad (4.4)$$

where κ is an increasing function of l . It is interesting to note the strong dependence of Γ on l which shows that the degree of anisotropy is crucial. In particular we see that the (non-rigorous) results by Bondi in [6] can be violated by anisotropic steady states. Indeed, Bondi considers isotropic matter models for which $\rho \geq 0$, $\rho \geq p$, or $\rho \geq 3p$, and gets 0.97, 0.86 and 0.70 respectively as upper bounds of $2M/R_1$. Since for Vlasov matter $\rho > p$, we see that the second bound is violated when l is large, i.e., the degree of non-isotropy is large, cf. the third case in Figure 15. For shells this bound is violated also when l is small as we saw in Figure 12. The degree of anisotropy in this case is large for any $l \geq 0$, since $p/\rho \rightarrow 0$ as $y(0) \rightarrow 0$, cf [2].

By taking l larger we get numerical evidence that also non-shells can have Γ arbitrary close to $8/9$, i.e., $\kappa(l) \rightarrow 8/9$, as $l \rightarrow \infty$, but still $\kappa(l) < 8/9$ for any l . In view of this claim and the claim made in the previous paragraph for shells, we find that the most important insight from our simulations in connection to Buchdahl's inequality is the following claim:

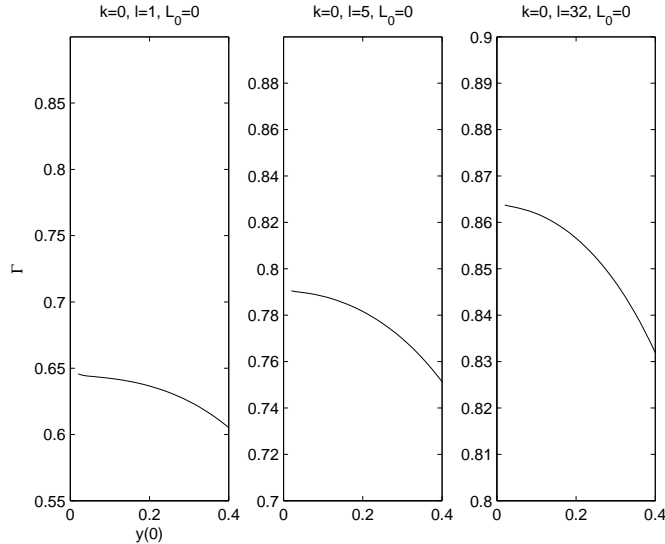


Figure 15: Γ versus $y(0)$ for non-shells

Any static solution of the Einstein-Vlasov system satisfies

$$\Gamma < \frac{8}{9}. \quad (4.5)$$

As mentioned above, the result in [2] shows that the inequality is sharp for shells and our numerical simulations indicate that it is also sharp for non-shells. It is an interesting and important problem to prove (4.5) in full generality.

5 Spirals in the (R, M) diagram

As we discussed in Section 2 for a fixed ansatz of the form (2.15) there exists a one-parameter family of corresponding non-trivial static solutions which are parameterized by $y(0) \in]0, 1[$ where $y = e^\mu/E_0$. One can now ask how for example the ADM mass M and the radius of the support R change along such a family. More specifically, one can plot for each $y(0)$ the resulting values for R and M to obtain a curve which reflects how radius and mass are related along such a one-parameter family of steady states. As a first example we choose $l = 0 = L_0$ and $k = 0$ in (2.22), i.e., an isotropic

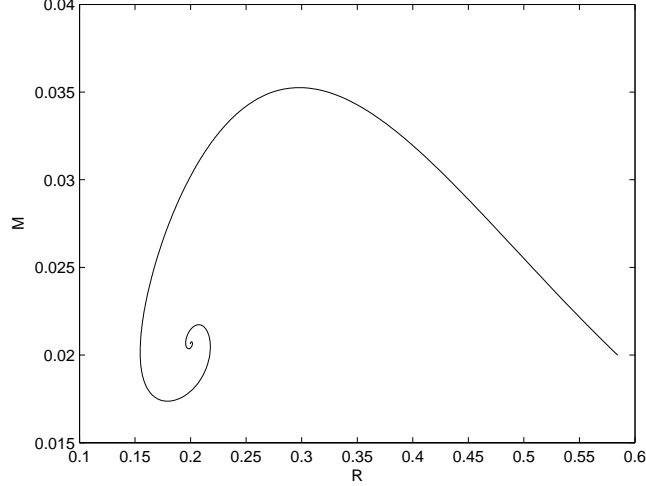


Figure 16: (R, M) spiral for $k = 0$, $l = 0$, $L_0 = 0$, $0.01 \leq y(0) \leq 0.95$

case, which results in the curve shown in Figure 16. We will discuss possible conclusions from such curves in more detail below, but note that there are possibly many steady states (or none at all) which have a given ADM mass and differ in radius.

As a matter of fact, for the isotropic case one can show that such radius-mass curves always have a spiral form. The following theorem easily follows from the corresponding result established by Makino for static, spherically symmetric solutions of the Einstein-Euler system under suitable assumptions on the macroscopic equation of state $p = p(\rho)$, cf. [11, Thm. 1]. For this theorem we parameterize our one-parameter family of steady states via the inverse of the central pressure, i.e., we define $\epsilon := \frac{3}{c_0 g_{3/2}(y(0))}$; notice that $g_{3/2}$ is one-to-one on $]0, 1]$ and $\epsilon \rightarrow 0$ iff $y(0) \rightarrow 0$.

Theorem 2 *Consider an isotropic ansatz of the form (2.15), i.e., $l = 0 = L_0$, and assume that the conditions on ϕ specified in (2.21) hold. Then as $\epsilon \rightarrow 0$,*

$$\begin{pmatrix} R(\epsilon) \\ M(\epsilon) \end{pmatrix} = \begin{pmatrix} R_S \\ M_S \end{pmatrix} + \epsilon^{\gamma_1} BJ(\gamma_2 \ln \epsilon) b + o(\epsilon^{\gamma_1}).$$

Here $R(\epsilon)$ and $M(\epsilon)$ denote the radius of the support and the ADM mass of the steady state corresponding to the parameter ϵ , R_S and M_S are positive

constants, B is a non-singular matrix,

$$J(\theta) := \begin{pmatrix} \cos \theta & -\sin \theta \\ \sin \theta & \cos \theta \end{pmatrix}$$

is a rotation by the angle $-\theta$, $b \in \mathbb{R}^2 \setminus \{0\}$, and γ_1, γ_2 are positive constants.

Proof. The definition of m in (2.7) together with the Tolman-Oppenheimer-Volkoff equation (2.12) in the isotropic case with (2.9) and (2.8) substituted in give the following system of equations:

$$\frac{dm}{dr} = 4\pi r^2 \rho, \quad (5.1)$$

$$\frac{dp}{dr} = -(\rho + p) \frac{m + 4\pi r^3 p}{r^2(1 - 2m/r)}. \quad (5.2)$$

Moreover,

$$\rho = c_0 (g_{3/2}(y) + g_{1/2}(y)),$$

where the right hand side is a strictly decreasing function of $y \in]0, 1]$ which converges to infinity as $y \rightarrow 0$. If we denote its inverse by

$$\sigma : [0, \infty[\rightarrow]0, 1], \quad \rho \mapsto y,$$

we find that the pressure p is related to the energy density ρ through an equation of state

$$p = P(\rho) := \frac{c_0}{3} g_{3/2}(\sigma(\rho)). \quad (5.3)$$

The equations (5.1), (5.2), (5.3) now provide a closed system of equations which describes an isotropic Einstein-Vlasov steady state purely in terms of macroscopic quantities and a macroscopic equation of state. This system also arises from the static, spherically symmetric Einstein-Euler system. It describes a gaseous star and is studied in [11]. Hence to prove the theorem above we only have to show that our equation of state (5.3) satisfies the assumptions made in [11], and then we can invoke the corresponding result established there.

Firstly, $P = P(\rho)$ is a smooth function of $\rho > 0$, since $\rho > 0$ iff $y \in]0, 1[$ iff $p > 0$ we have $P(\rho) > 0$ for $\rho > 0$ and since $\rho \rightarrow 0$ iff $y \rightarrow 1$ iff $p \rightarrow 0$ it follows that $P(\rho) \rightarrow 0$ as $\rho \rightarrow 0$. Moreover, by (2.20),

$$\frac{dP}{d\rho} = \frac{dP}{dy} \frac{dy}{d\rho} = \frac{1}{3} \frac{4g_{3/2}(y) + 3g_{1/2}(y)}{4g_{3/2}(y) + 5g_{1/2}(y) + g_{-1/2}(y)} < \frac{1}{3} < 1$$

for all $0 < \rho < \infty$, and also $\frac{dP}{d\rho} > 0$, so that the assumption (A.0) in [11] is satisfied.

The assumption (A.1) in [11], namely that for $\rho \rightarrow 0$,

$$\frac{\rho}{P} \frac{dP}{d\rho} = \gamma + O(\rho^{\gamma-1})$$

with some constant $4/3 < \gamma < 2$, is needed only to make sure that the solutions of the system (5.1), (5.2), (5.3) have finite radius. Since we know this a priori by the assumption (2.21), we need not check this condition. But using the results of [15] one finds that (A.1) holds with $\gamma = (k+5/2)/(k+3/2)$ which lies in the required interval $]4/3, 2[$ iff $-1/2 < k < 3/2$, and this is precisely the assumption on k in (2.21) for $l = 0$.

The final condition (A.2) which we need to check is that the limit

$$\lim_{\rho \rightarrow \infty} \frac{P}{\rho} = \alpha_0 \in]0, 1[$$

exists, and that there exists some non-decreasing function ω such that

$$\left| \frac{P}{\rho} - \alpha_0 \right| \leq \omega \left(\frac{1}{P} \right) \quad \text{and} \quad \int_0^1 \frac{\omega(x)}{x} dx < \infty.$$

For this it is useful to introduce the functions

$$h_j(y) := \int_y^1 \phi(\eta) (\eta^2 - y^2)^j d\eta, \quad y \in [0, 1],$$

so that

$$g_j(y) = y^{-(2j+1)} h_j(y), \quad y \in]0, 1].$$

Then

$$\lim_{\rho \rightarrow \infty} \frac{P}{\rho} = \frac{1}{3} \lim_{y \rightarrow 0} \frac{g_{3/2}(y)}{g_{3/2}(y) + g_{1/2}(y)} = \frac{1}{3} \lim_{y \rightarrow 0} \frac{h_{3/2}(y)}{h_{3/2}(y) + y^2 h_{1/2}(y)} = \frac{1}{3};$$

note that $h_{3/2}(0) > 0$. Moreover,

$$\begin{aligned} \left| \frac{P}{\rho} - \frac{1}{3} \right| &= \frac{1}{3} \frac{g_{1/2}(y)}{g_{3/2}(y) + g_{1/2}(y)} \leq \frac{1}{3} \frac{g_{1/2}(y)}{g_{3/2}(y)} \\ &= \frac{1}{3} \left(\frac{c_0}{3} \right)^{1/2} \frac{g_{1/2}(y)}{(g_{3/2}(y))^{1/2}} \frac{1}{(c_0 g_{3/2}(y)/3)^{1/2}} \\ &= \frac{1}{3} \left(\frac{c_0}{3} \right)^{1/2} \frac{g_{1/2}(y)}{(g_{3/2}(y))^{1/2}} \frac{1}{\sqrt{P}}. \end{aligned}$$

If we can show that $g_{1/2}(y) (g_{3/2}(y))^{-1/2}$ is bounded then the condition (A.2) holds with $\alpha = 1/3$ and $\omega(x) = c\sqrt{x}$, where $c > 0$ is a suitable constant. Now

$$\frac{g_{1/2}(y)}{(g_{3/2}(y))^{1/2}} = \frac{h_{1/2}(y)}{(h_{3/2}(y))^{1/2}},$$

and the functions $h_{1/2}$ and $h_{3/2}$ are continuous and positive on $[0, 1[$. Hence it remains to show that the above fraction has a finite limit as $y \rightarrow 1$. Let us denote $\varepsilon := 1 - y^2 \rightarrow 0$ as $y \rightarrow 1$. Then by [15, (3.18)],

$$\frac{h_{1/2}(y)}{(h_{3/2}(y))^{1/2}} = \frac{\frac{1}{2}c_{k,1/2}\varepsilon^{k+3/2} + O(\varepsilon^{k+3/2+\delta})}{\left(\frac{1}{2}c_{k,3/2}\varepsilon^{k+5/2} + O(\varepsilon^{k+5/2+\delta})\right)^{1/2}} \rightarrow 0$$

as $\varepsilon \rightarrow 0$, since $k + 3/2 > (k + 5/2)/2$ which is equivalent to $k > -1/2$. The latter holds by the assumption on k in (2.21), and the proof is complete. \square

The theorem above is restricted to isotropic steady states, but numerically we have so far found no microscopic equation of state, isotropic or not, which does not lead to a radius-mass spiral, although for sufficiently anisotropic cases the spiral becomes rather deformed. Corresponding examples are given in Figures 17 and 18.

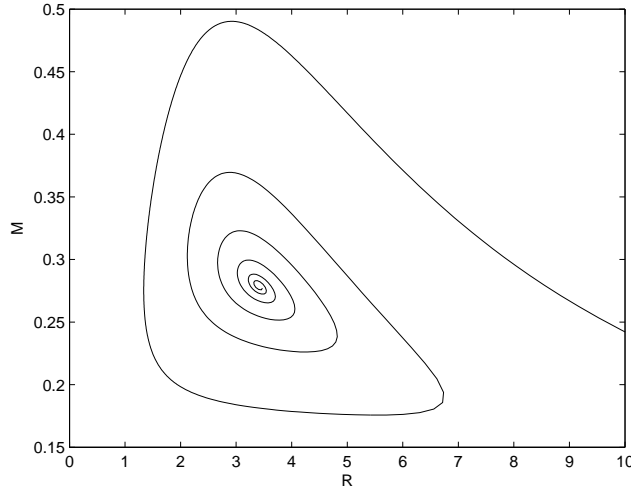


Figure 17: (R, M) spiral for $k = 0$, $l = 10.5$, $L_0 = 0$, $0.01 \leq y(0) \leq 0.99$

The sharp corner in Figure 18 is a genuine feature of this curve and can be explained as follows. For $L_0 > 0$ the steady state can consist of several

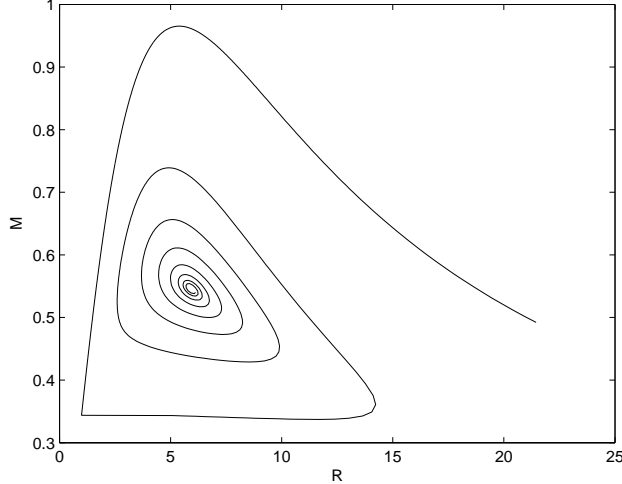


Figure 18: (R, M) spiral for $k = 1$, $l = 5$, $L_0 = 2.0$, $0.01 \leq y(0) \leq 0.99$

shells of matter separated by vacuum. For $y(0)$ close to 1 only a single shell is present, but at a certain value of $y(0)$ a second shell appears at a certain radius which causes the outer radius of the steady state to increase discontinuously while the mass remains more or less constant; recall that $\rho(r) > 0$ iff $y(r)\sqrt{1 + L_0/r^2} < 1$, and although $y(r)\sqrt{1 + L_0/r^2}$ depends continuously on $y(0)$ the region where the former condition holds can change discontinuously.

We conjecture that such radius-mass spirals are a general feature of one-parameter families of steady states of the spherically symmetric Einstein-Vlasov system. This is surprising, since it is by no means true for the Vlasov-Poisson system. For example, the polytropic ansatz

$$f(r, w, L) = (E_0 - E)_+^k L^l$$

with $k, l > -1$, $k + l > -1/2$, and $k < 3l + 7/2$ is known to lead to steady states with finite mass and compact support; the particle energy E is given in terms of the gravitational potential $U(r)$ by

$$E = U(r) + \frac{1}{2}(w^2 + L/r^2).$$

If we keep k and l fixed we obtain a one-parameter family of steady states which is conveniently parameterized by $y(0) = E_0 - U(0)$. The resulting

equation for $y = E_0 - U$ is

$$\frac{1}{r^2}(r^2 y')' = -4\pi c_{k,l} r^{2l} y_+^{k+l+3/2},$$

where $c_{k,l}$ is some positive constant. One can obtain any solution of this equation by properly rescaling a fixed, particular one, say, the one with $y(0) = 1$. Using this fact it is easy to show that if $k - l - 3/2 \neq 0$ there exists for each prescribed mass $M \in]0, \infty[$ exactly one steady state in the family with that mass, and the relation between radius and mass is

$$M = R^{(k-l-3/2)/(k+l+1/2)}.$$

If $k - l - 3/2 = 0$ all steady states of the family have the same mass. In the relativistic case the picture is very different, even for the same type of ansatz. If the prescribed mass is too large or too small there does not seem to be a corresponding steady state in the family, while for masses in the intermediate range there are in general more than one steady state of that mass. For the mass $M = M_S$ corresponding to the focus of the spiral, cf. Theorem 2, there are infinitely many steady states of that mass, which differ in their radii.

Further interest in these radius-mass spirals comes from the fact that in astrophysical investigations conclusions about stability of the steady states in question are often drawn from them via the ‘‘Poincaré turning point principle’’: If one knows from somewhere that one steady state on the upper part of the spiral to the right of its first maximum is stable then it is claimed that all steady states up to the first maximum of M along the spiral are stable, and that towards the left of that point stability is lost. We can unfortunately not claim to understand the arguments by which this principle is supported, in particular not in the case of an infinite dimensional dynamical system such as the Einstein-Vlasov system, and we are not aware of any rigorous mathematical result on stability for this system beyond the preliminary results in [18]. However, numerically we found in [4] that along such a one-parameter family of steady states stability is lost if the so-called binding energy passes its maximum, and numerically it turns out that this happens at the same parameter value where M attains its maximum. Hence the prediction of the turning point principle agrees with the numerical stability analysis in [4].

Above we showed analytically that radius-mass spirals are not always present in the Newtonian case. An example where numerically one does find a radius-mass spiral is the so-called King model where

$$f(r, w, L) = (e^{E_0 - E} - 1)_+.$$

This model is important in astrophysics. According to the turning-point principle outlined above there should be a transition from stable to unstable steady states along the corresponding one-parameter family, but it has been proven in [8] that all steady states of King type are non-linearly stable; the analogous result for the so-called relativistic Vlasov-Poisson system has been established in [10]. It is conceivable that in the non-relativistic case one must plot other quantities instead of radius and mass to apply the turning-point principle, but if one for example plots the radius versus the total energy for the King model again a spiral arises, which in view of [8] does not agree with the prediction of the turning-point principle.

We conclude this section by emphasizing that the mathematically rigorous relation—if any—of such radius-mass spirals to stability properties of the steady states seems a very interesting and non-trivial problem in general and for the Einstein-Vlasov system in particular. An also very interesting problem is to prove that radius-mass spirals are present for the Einstein-Vlasov system in the anisotropic case as well, as our numerical experiments seem to indicate.

References

- [1] H. ANDRÉASSON, The Einstein-Vlasov System/Kinetic Theory. *Living Rev. Relativ.* **8** (2005)
- [2] H. ANDRÉASSON, On static shells and the Buchdahl inequality for the spherically symmetric Einstein-Vlasov system. Preprint, gr-qc/0605151
- [3] H. ANDRÉASSON, On the Buchdahl inequality for spherically symmetric static shells. Preprint, gr-qc/0605097
- [4] H. ANDRÉASSON, G. REIN, A numerical investigation of the stability of steady states and critical phenomena for the spherically symmetric Einstein-Vlasov system. *Class. Quantum Grav.* **23**, 3659–3677 (2006)
- [5] J. BATT, W. FALTENBACHER, E. HORST, Stationary spherically symmetric models in stellar dynamics. *Arch. Rational Mech. Anal.* **93**, 159–183 (1986)
- [6] H. BONDI, Massive spheres in general relativity. *Proc. of the Royal Soc. of London. Series A, Mathematical and Physical Sciences* **282**, 303–317 (1964)

- [7] H. A. BUCHDAHL, General relativistic fluid spheres. *Phys. Rev.* **116**, 1027–1034 (1959)
- [8] Y. GUO, G. REIN, A non-variational approach to nonlinear stability in stellar dynamics applied to the King model. *Comm. Math. Phys.*, to appear, math-ph/0602058
- [9] J. GUVEN, N. Ó MURCHADHA, Bounds on $2m/R$ for static spherical objects. *Phys. Rev. D* **60**, 084020 (1999)
- [10] M. HADŽIĆ, G. REIN, Global existence and nonlinear stability for the relativistic Vlasov-Poisson system in the gravitational case. *Indiana University Math. J.*, to appear, math-ph/0607012
- [11] T. MAKINO, On the spiral structure of the (R, M) -diagram for a stellar model of the Tolman-Oppenheimer-Volkoff equation. *Kunkcialaj Ekvacioj* **43**, 471–489 (2000)
- [12] G. REIN, Static solutions of the spherically symmetric Vlasov-Einstein system. *Math. Proc. Camb. Phil. Soc.* **115**, 559–570 (1994)
- [13] G. REIN, Static shells for the Vlasov-Poisson and Vlasov-Einstein systems. *Indiana University Math. J.* **48**, 335–346 (1999)
- [14] G. REIN, A. D. RENDALL, Smooth static solutions of the spherically symmetric Vlasov-Einstein system. *Ann. de l'Inst. H. Poincaré, Physique Théorique* **59**, 383–397 (1993)
- [15] G. REIN, A. D. RENDALL, Compact support of spherically symmetric equilibria in non-relativistic and relativistic galactic dynamics. *Math. Proc. Camb. Phil. Soc.* **128**, 363–380 (2000)
- [16] A. D. RENDALL, An introduction to the Einstein-Vlasov system. *Banach Center Publ.* **41**, 35–68 (1997)
- [17] J. SCHAEFFER, A class of counterexamples to Jeans' theorem for the Vlasov-Einstein system. *Comm. Math. Phys.* **204**, 313–327 (1999)
- [18] G. WOLANSKY, Static solutions of the Vlasov-Einstein system. *Arch. Rational Mech. Anal.* **156** 205–230 (2001)